PROCEEDINGS OF THE INTERNATIONAL CONFERENCE
NANOMATERIALS: APPLICATIONS AND PROPERTIES
Vol. **4** No 1, 01PISERE02(3pp) (2015)

Ion Recrystallization and Spheroidization in Amorphous AlN-TiB_2-$TiSi_2$ as a Result of Annealing and Subsequent Implantation by Negative ion Au^-

A.O. Demianenko[1], O.V. Bondar[1], A.A. Goncharov[1], J. Partyka[2], S. Borba[1]

[1] *Sumy State University, 2, Rymsky Korsakov Str., 40007 Sumy, Ukraine*
[2] *Politechnika Lubelska, 38D, Nadbystrzycka, 20-618, Lublin, Poland*

(Received 15 July 2015; published online 29 August 2015)

This paper presents new results on investigation of the influence of Au- negative ion beam implantation and thermal annealing under 900 °C and 1300 °C on structure and characteristics of AlN-TiB_2-$TiSi_2$ coatings prepared by magnetron sputtering. Using scanning electron microscope (SEM) with microanalysis (EDS), atomic force microscopy (AFM), X-Ray diffraction (XRD), high-resolution transmission electron microscopy (HRTEM) investigated the crystal structure, surface topography, microstructure were characterized.

Keywords: Annealing, Implantation, Amorphous, Nanocomposite, Phases, Ions Au^-.

PACS numbers: 61.05.cm, 61.46.Hk, 62.20.Qp.68.37.Hk, 81.15. – z

1. INTRODUCTION

The development of hard coatings, defined by hardness values above 40 GPa, has increased significaantly during the last 15 years because of the interest in scientific and industrial applicatins. These hard coatings possess an unusual combination of mechanical and chemical properties, such as high fracture toughness, high oxidation resistance and high thermal and chemical stability [1-10].

2. EXPERIMENTAL AND DETAILS

The high-temperature AlN-TiB_2 composite with addition of $TiSi_2$ which used as sputtered material. The coatings were annealed at 900 ºC and 1300 ºC.

To study the effect of ion bombardment (ion implantation Au c 40 keV to a dose of 10^{17} cm^2) irradiated coating were recorded at grazing incidence angle of the smallest 2º when the informative depth study of less than 100 nm.

To analyze the surface morphology of the samples (with microanalysis) was applied SEM JEOL-7000F with microanalysis and accelerating voltage 20 keV.

To determine the surface topography with high resolution used atomic force microscope (AFM).

X-ray diffraction researches of samples were performed using an X-ray diffractometer RINT-2500 V using a position-sensitive proportional counter (PSPC / MDGT). Operating voltage and current X-ray diffractometer were 40 kV and 300 mA, respectively. Measurements were made at angles of 3°, 10°, 30°.

Optical microscope, additional SEM, roughness gauge obtained by 3D Laser Scanning Microscope VK-X100/X200 Series.

The HRTEM images were conducted by an electron microscope JEOL JEM-2100F in the bright and dark field with electron energy of 200 keV.

3. RESULTS AND DISCUSSION

The fractography and fracture topography of AlN-TiB_2-$TiSi_2$ coatings with thickness of about 7 μm are shown in Fig. 1 a, b. As a result of the image of the surface of the coating, it can be seen that during the deposition of the coating it was in areas with a drop size and achieved in a fraction of a few microns, and the absence of cracks indicates a good quality of coating.

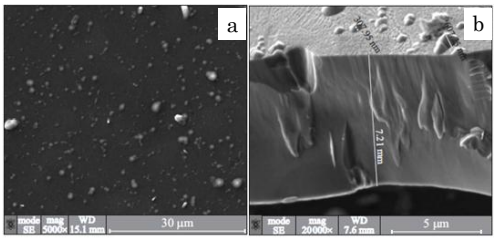

Fig. 1 – The experimental setup for the determination of the adhesion / cohesion strength. FN- value of the normal load, FT- friction force

Surface exhibit heterogeneity on the surface is determined by the local inhomogeneity of multielement structure (Fig. 2).

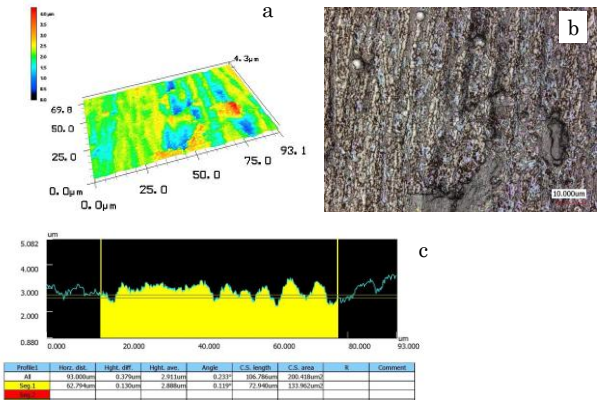

Fig. 2 – Surface of the coating after annealing at 1300 ºC and distribution profile of 3D laser+ optical method: a) surface of the coating; b) image in thermal contrast c) image of roughness

The obtained results of elemental analysis of the composition in the form of maps of the distribution of

elements in elemental contrast and bright-field given in Figure 3. Uniform distribution observed for C, Al, Ti, Si, Fe, in contrast oxygen, which is higher near the surface. Well visible trace Au, extending deep cover with a concentration of about 0,4 at. %.

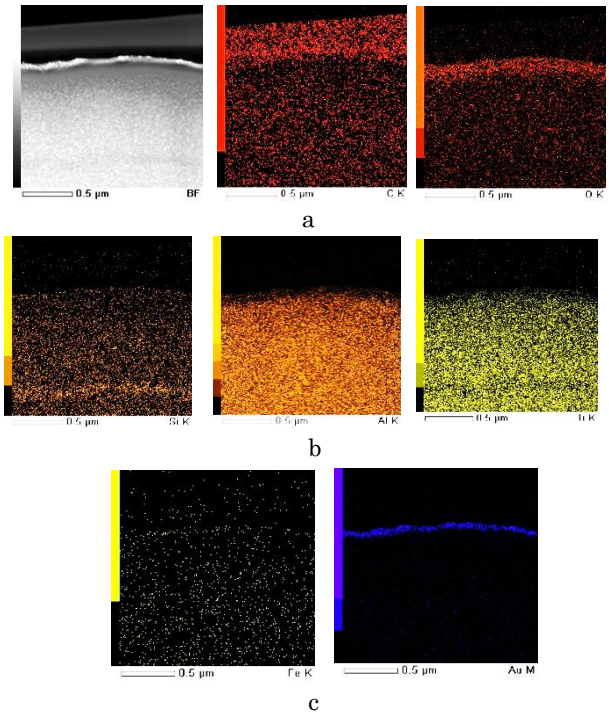

Fig. 3 – Results of elemental analysis: a) B, C, O; B) Si, Al, Ti, a) Fe, Au in the form of maps of distribution of elements across the sample in elemental contrast

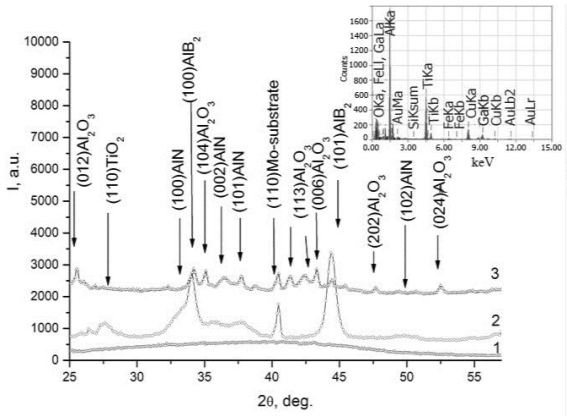

Fig. 4 – Radiographs of AlN-TiB_2-$TiSi_2$ based coatings, obtained from the coating of molybdenum substrate in the initial state is a curve 1, after high-temperature annealing at a temperature of 900 °C is a curve 2 and 1300 °C - curve 3

The formation of the amorphous structure of the coating as a result of measurement using XRD, TEM, HRTEM analysis. Short-range evaluation order was produced in the coatings using the relation:

$$Rm = \frac{10}{\Delta s}$$

where Δs – width of the first wide angle "halo figurative" curve in the coordinates of "intensity-scattering vector s" (modulus of scattering vector $s = |s| = 4\pi\sin\theta/\lambda$). The ordering regions: $R_m \sim 10$ A = 1 nm.

The expression (1) follows from the fact that correlation (value range order) is inversely proportional to Δs:

$$Rm = \frac{2\pi^3 \cdot z^2}{6.25\Delta s},$$

where z – index of maximum. For the first peak ($z = 1$), $Rm = 10/\Delta s$ were formed in the coating, are less noticeable that AlB_2. Also it was found TiO_2, AlN phases and "possible" SiO_2 in small quantities. The formation of AlB_2 and Al_2O_3 crystallites occur due to the highest heat of the formation of these phases.

As we can see from the image 5a, can be seen cross section of specimen. On figure 5b can be seen scanning transmission electron microscope image of the surface.

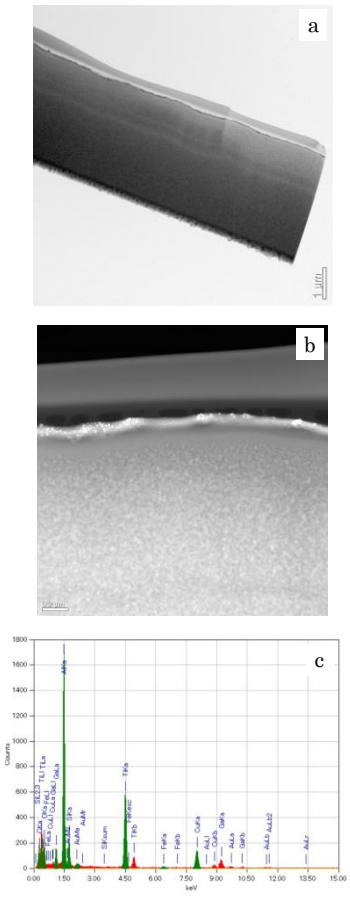

Fig. 5 – a) Cross sectional TEM-specimen of coating side; b) HAADF-STEM Image; c) EDS Spectrum.

After the high temperature annealing and subsequent ion implantation in the coating formed three characteristic zones: close to the surface – implantation zone with thickness of about 40 nm, with dolped implanted gold, as seen from visualizing results of high resolution transmission electron microscopy.

On figure 7, it can be seen crystalline structural state (with a thickness ~ 1 μm). As is was shown on investigation of structural-phase state of coatings with different amount of coatings its forms textured 2-levels grain structure in which grains of submicron sizes (up to 0,5 μm) fragmented by small-angle (with angles of deorintation to 5 °C).

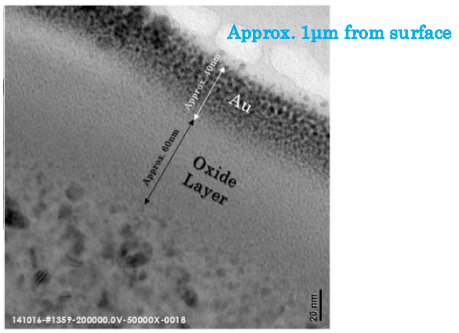

Fig. 6 – TEM-image of coating with implantation and annealing at 1300 °C

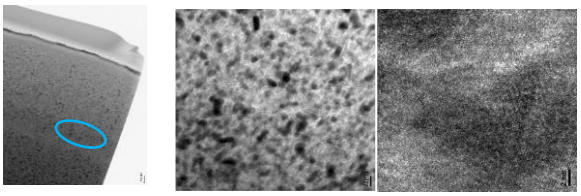

Fig. 7 – High-resolution electron micrographs with microdiffraction of coating at a depth of 1 µm from the surface

REFERENCES

1. D.P. Datta, Y. Takeda, H. Amekura, *Appl. Surf. Sci.* **310**, 164 (2014).
2. A.D. Pogrebnjak, V.M. Beresnev, *Nanocoatings, Nanosystems, Nanotechnologies* (Benth. Sci. Publ. 2012).
3. A.D. Pogrebnjak, A.P. Shpak, N.A. Azarenkov, V.M. Beresnev, *Phys. Usp.* **52**, 29 (2009).
4. A.D. Pogrebnjak, G. Abadias, O.V. Bondar, *Acta Phys. Pol. A* **125**, 1284 (2014).
5. A.D. Pogrebnjak, A.A. Bagdasaryan, I.V. Yakushenko, V.M. Beresnev, *Rus. Chem. Rev.* **83**, 1027 (2014).
6. A.D. Pogrebnjak, D. Eyidi, G. Abadias, O.V. Bondar, *Mat. Chem. Phys.* **147**, 1079 (2014).
7. A.D. Pogrebnjak, I.V. Yakushenko, A.A. Bagdasaryan.
8. A.D. Pogrebnjak, S.N. Bratushka, V.M. Beresnev, N. Levintant-Zayonts, *Usp. Khim.* **82**, 1135 (2013).
9. V. Ivashchenko, S. Veprek, A.D. Pogrebnjak, B.A. Postolnyi, *Sci. Technol. Adv. Mat.* **15**, 025007 (2014).
10. A.D. Pogrebnjak, G. Abadias, A.A. Demianenko, et al., *Acta Phys. Pol. A* **125** No6, 1287 (2014).
11. B.O. Postolnyi, O.V. Bondar, Yu.A. Kravchenko, A.P. Shypylenko, O.V. Sobol', V.M. Beresnev, P. Wegizek, K. Smirnova, Ya. Kravchenko, *Proc. NAP* **1** No1, 01FNC06 (2012).
12. A.O. Demianenko, V.M. Rogoz, *Proc. NAP* **2** No1, 01NTF38 (2013).
13. A. Demianenko, J. Partyka, K.O. Belovol, et al., *Proc. NAP* **3** No1 (2014).
14. A.D. Pogrebnyak, V.N. Borisyuk, A.A. Bagdsaryan, et al., *Proc. NAP* **1** No2, 02NFC27 (2012).